Parasitology International 64 (2015) 609–621

Contents lists available at ScienceDirect

Parasitology International

journal homepage: www.elsevier.com/locate/parint

Skin lesions on yellowfin tuna *Thunnus albacares* from Gulf of Mexico outer continental shelf: Morphological, molecular, and histological diagnosis of infection by a capsalid monogenoid

Stephen A. Bullard [a,b,*], Matthew R. Womble [a], Margaret K. Maynard [a], Raphael Orélis-Ribeiro [a], Cova R. Arias [c]

[a] Aquatic Parasitology Laboratory, School of Fisheries, Aquaculture, and Aquatic Sciences (SFAAS), Auburn University, 203 Swingle Hall, Auburn, AL 36849, USA
[b] Auburn University Center for Aquatic Surveillance and Health, SFAAS, CASIC 559 Devall Drive, Auburn AL 36832, USA
[c] Aquatic Microbiology Laboratory, SFAAS, Auburn University, CASIC 559 Devall Drive, Auburn AL 36832, USA

ARTICLE INFO

Article history:
Received 1 April 2015
Received in revised form 24 July 2015
Accepted 11 August 2015
Available online 13 August 2015

Keywords:
Skin lesion
Tuna
Gulf of Mexico
28S
Pathology

ABSTRACT

We characterize lesion-associated capsaline infections on yellowfin tuna, *Thunnus albacares*, in the Gulf of Mexico by comparing our specimens with published descriptions and museum specimens ascribed to *Capsala biparasiticum* and its synonyms: vouchers of *C. biparasiticum* from parasitic copepods; the holotype of *Capsala neothunni*; and vouchers of *Capsala abidjani*. Those from parasitic copepods differed by having a small, rounded body, large anterior attachment organs, closely spaced dorsomarginal body sclerites, small testes, and a short and wide testicular field. No morphometric feature in the holotype of *C. neothunni* ranged outside of that reported for the newly-collected specimens, indicating conspecificity of our specimens. The specimens of *C. abidjani* differed by having a large anterior attachment organ, few and dendritic testes, and a short, wide testicular field. Large subunit ribosomal DNA (28S) sequences grouped our specimens and *Capsala* sp. as sister taxa and indicated a phylogenetic affinity of *Nasicola klawei*. The haptoral attachment site comprised a crater-like depression surrounded by a blackish-colored halo of extensively rugose skin, with abundant pockmarked-like, irregularly-shaped oblong or semi-circular epidermal pits surrounding these attachment sites. Histology confirmed extensive folding of epidermis and underlying stratum laxum, likely epidermal hyperplasia, foci of weak cell-to-cell adhesions among apical malpighian cells as well as that between stratum germinativum and stratum laxum, myriad goblet cells in epidermis, rodlet cells in apical layer of epidermis, and lymphocytic infiltrates and melanin in dermis. The present study comprises (i) the first published report of this parasite from yellowfin tuna captured in the Gulf of Mexico–NW Atlantic Ocean Basin, (ii) confirmation of its infection on the skin (rather than on a parasitic copepod), (iii) the first molecular data for this capsaline, and (iv) the first observations of histopathological changes associated with a capsalid infection on a wild-caught epipelagic fish.

1. Introduction

Much remains to be explored regarding the basic biology, biodiversity, host specificity, and geographic distributions of ectoparasites that infect wide-ranging epipelagic marine fishes, especially tunas (*Thunnus* spp.) [1]. This lack of information is a barrier to understanding the ecology and evolutionary interrelationships of the parasites themselves and impedes a more holistic understanding of their hosts' biology. For example, parasites of pelagic fishes can be used as biological tags indicative of stock structure [2] or to explore host–parasite relationships in nature that inform best practices for the health management and biosecurity of tunas raised in sea cages [3–5]. Even more fundamental, we know little about how these parasites affect health of their wild hosts, e.g., no previous study has detailed a lesion attributable to an ectoparasitic monogenoid on a wild-caught epipelagic fish.

Capsala spp. comprise commonly observed and collected ectoparasitic flatworms, including 36 accepted species [6,7] (*Capsala* is herein provisionally considered a senior subjective synonym of *Caballerocotyla* Price, 1960). They are among the most highly-visible and widely-reported of marine fish ectoparasites due to their large size and durability, i.e., they remain attached, intact, and visible on fishes for many hours after the fish has been killed and kept on ice, and due to the high recreational and commercial value of the hosts they infect, i.e., "big game fishes" such as tunas (Scombridae), jacks (Carangidae), and billfishes (Istiophoridae, Xiphiidae). *Capsala biparasiticum* (Goto, 1894) Price, 1938 reportedly infects the buccal cavity epithelium of several tunas (*Thunnus* spp.) and the dorsum of parasitic copepods infecting yellowfin tuna, *Thunnus albacares*, in the Pacific Ocean (Table 1). This particular capsalid is interesting both taxonomically

* Corresponding author at: Aquatic Parasitology Laboratory, School of Fisheries, Aquaculture, and Aquatic Sciences, 203 Swingle Hall, Auburn University, Auburn, AL 36849, USA.
E-mail address: ash.bullard@auburn.edu (S.A. Bullard).

http://dx.doi.org/10.1016/j.parint.2015.08.005
1383-5769/

Table 1
Host and geographic locality records for *Capsala biparasiticum* (Goto, 1894) Price, 1939 (Capsalidae: Capsalinae) and putative conspecifics infecting tunas.

Fish host	Copepod host/site of infection	Capsalid body size (maximum reported)	Locality	Types, voucher materials	Reference
***Thunnus albacares*, yellowfin tuna** (as "*Thynnus albacora*")	"Carapace of a copepod, probably of the genus *Parapetalus*, parasitic on the gill"	6 mm × 3 mm	NW Pacific Ocean (landed at Misaki, Japan)	Present disposition indeterminate, presumably no longer extant	Goto [8] (as *Tristomum biparasiticum*); Price [9]
T. albacares	Inner surface of opercle (buccal cavity)	8 mm × 5 mm	NW Gulf of Mexico off Louisiana (27°11.43'N; 90° 01.37'W)	**USNM 1283167-69**	**Present study**
T. albacares, (as *Neothunnus macropterus*)	"Firmly attached to carapace of copepods (*Elytrophora* sp.) found in gills"	2 mm × 2 mm	NW Pacific Ocean (2°14′N; 159°59′W); (off Christmas Island)	**USNPC 38134** (2 vouchers); **HWML 44308*** (1 voucher)	Iverson and Hoven [10] (as *Capsala biparasitica*); **present study**
T. albacares, (as *Neothunnus macropterus*)	"Gills"	7 mm × 3 mm	Pacific Ocean (off Hawaii)	**USNPC 63569**	Yamaguti [11] (as *Capsala neothunni*); **present study**
T. albacares, (as *Neothunnus macropterus*)	"Dorsal surface of a caligoid copepod"	7 mm × 4 mm	Pacific Ocean (off Hawaii)	None reportedly deposited (NRD)	Yamaguti [11] (as *Capsala biparasitica*)
T. albacares (as *Parathunnus sibi*)	"Dorsal surface of caligoid copepod"	7 mm × 4 mm	Pacific Ocean (off Hawaii)	NRD	Yamaguti [11] (as *Capsala biparasitica*)
T. albacares	"Internal face of branchial gill-covers"	11 mm × 5 mm	NE Atlantic Ocean (Gulf of Guinea)	NRD	Bussiéras and Baudin-Laurencin, [12] (as *Caballerocotyla abidjani*)
T. albacares	"Internal face of branchial gill-covers"	8 mm × 4 mm	NE Atlantic Ocean (between 8 and 13°N; 19°E)	NRD	Bussieras [13] (as *Caballerocotyla abidjani abidjani* and *Caballerocotyla abidjani microcotyla*); Vassiliadès [14]
***Thunnus obesus*, bigeye tuna**	"Internal face of branchial gill-covers"	8 mm × 4 mm	NE Atlantic Ocean (between 8 and 13°N; 19°E)	NRD	Bussieras [13] (as *Caballerocotyla abidjani abidjani* and *Caballerocotyla abidjani microcotyla*); Vassiliadès [14]
T. albacares	Unspecified	Not reported	Atlantic Ocean	NRD	Pozdnyakov [15] (as *Caballerocotyla abidjani*) (in Munday et al. 2003)
T. obesus	Unspecified	Not reported	Unspecified	NRD	Pozdnyakov [15] (in Munday et al. 2003)
***Thunnus maccoyii*, southern bluefin tuna**	Unspecified	Not reported	Unspecified	NRD	Pozdnyakov [15] (in Munday et al. 2003)
T. albacares	"Buccal cavity"	5 mm × 3 mm	SE Atlantic Ocean (landed at Mapelane, Mozambique)	**BMNH.1975.9.17.11-12** (2 specimens on 1 slide)	**Present study,** slide labeled as "*Caballerocotyla abidjani*" [13]
"Scombridae"	Unspecified	Not reported	Atlantic Ocean	NRD	Egorova [16] (as *Caballerocotyla abidjani*)
T. albacares	"Gills"	11 mm × 5 mm	SW Atlantic Ocean (off Brazil)	CHIOC 36612 A-C; 36613	Kohn and Justo [17] (as *Caballerocotyla neothunni*)

and ecologically, warranting morphological study of new and existing specimens as well as histopathological evaluation of infected tissues from wild-caught tunas. Regarding taxonomy, no type materials exist, no specimen has been collected from the type host or type locality, incomplete descriptions of capsalines from yellowfin tunas in other localities have created some typical taxonomic confusion, and molecular data are lacking for this and related capsalines that infect yellowfin tuna. Regarding host–parasite relationships, it is highly unusual for a monogenoid to infect an invertebrate or more than a single host in its life cycle, and, as previously mentioned, we are aware of no previous study that has provided information on the pathological effects of capsalid infections on a wild-caught tuna (Scombridae). Anecdotal observations by one of us (SAB) of ectoparasite infections on tunas indicates that gross lesions on tunas are uncommon, despite seemingly all wild-caught tunas being infected by specimens of at least one capsalid species.

During a sampling trip in the northern Gulf of Mexico's (GOM) outer continental shelf (OCS), we observed a striking, blackish-colored skin lesion on the inner surface of the operculum of yellowfin tunas infected by a capsaline (Figs. 1–5). Because these capsalines were nearly transparent in life, such an infection could easily be misinterpreted as being attributable to a non-infectious disease rather than a parasitic infection. Such misinterpretation is especially likely in light of recent anecdotal assertions that the 2010 *BP Deepwater Horizon* oil spill (DHOS) caused an array of "open skin lesions" on a spectrum of marine fishes in the GOM. Although these assertions have yet to be accompanied with defensible scientific evidence from parasitology, microbiology, mycology, immunology, or pathology, for example, they raised concern about GOM fish health. As such, studies detailing the etiology of gross lesions on GOM fishes are timely and contribute to helping differentiate lesions associated with putative infectious vs. putative non-infectious diseases.

We herein provide light and scanning electron microscopy observations of these capsalines from lesioned GOM yellowfin tuna. For taxonomic purposes, we make direct comparisons between our newly-collected specimens and previously collected specimens from yellowfin tuna. Phylogenetic analysis of sequence data from the large subunit ribosomal DNA (28S) helped inform the taxonomic identity and phylogenetic placement of our specimens. We also document gross and histopathological changes to the buccal cavity epithelium of these infected yellowfin tuna as well as furnish new knowledge about and summarize previous records of the parasite's distribution in nature by providing an updated list of hosts and geographic locality records. The present study comprises (i) the first published report of this parasite from yellowfin tuna captured in the Gulf of Mexico–NW Atlantic Ocean Basin, (ii) confirmation of its infection on the skin (rather than on a parasitic copepod), (iii) the first molecular sequence data for this

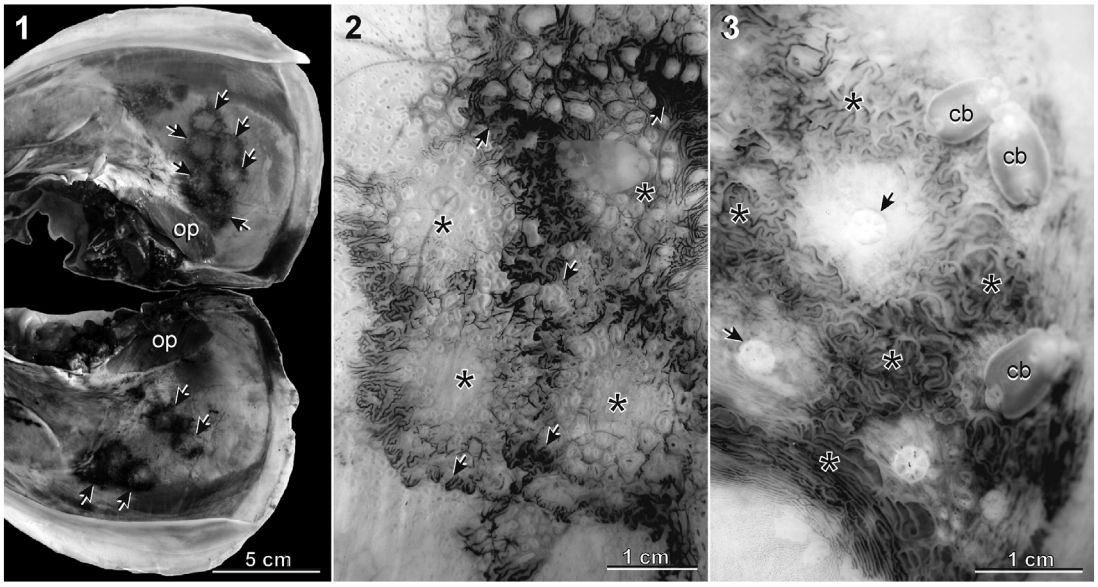

Figs. 1–3. Specimens of *Capsala* cf. *biparasiticum* (Goto, 1894) Price, 1938 (Monogenoidea: Capsalidae) from epithelial surface of inner surface of the operculum (immediately ventral to opercular pseudobranch) of yellowfin tuna, *Thunnus albacares* (Perciformes: Scombridae) captured in the north-central Gulf of Mexico's outer continental shelf. Scale bar value aside each bar. (1) Inner surface (buccal cavity) of excised, infected opercula (sinistral and dextral opercula at top and bottom of figure, respectively, with trailing edge of operculum at right) showing parasite attachment sites (arrows) in area immediately ventral to opercular pseudobranch (op). Note that haptoral attachment sites are opaque, encircled by a black, halo-like zone of skin. (2) Skin, *en vivo*, showing focal areas of melanin (arrows) associated with epidermis surrounding haptoral attachment sites (*); upper right attachment site accommodates an adult specimen of *C.* cf. *biparasiticum*, which is nearly transparent (in vivo). (3) Extensively rugose skin (*), post-fixation, associated with attached specimens (cb) of *C.* cf. *biparasiticum* as well as other sites (arrows) from where attached worms relocated or became detached during tissue processing. Note that skin rugosity is intense near haptoral attachment sites, suggesting that feeding activity of the worms may be closely associated with rugose skin (oral and haptoral ends of the worms are oriented top and bottom in figure, respectively).

capsaline, and (iv) the first observations of histopathological changes associated with a capsalid infection on a wild-caught epipelagic fish.

2. Materials and methods

Nineteen yellowfin tuna (53–129 cm caudal fork length) were captured from nearby the oil drilling tension leg platform *Atlantis* (north-central GOM, Green Canyon, 116 nautical miles (134 km) south/southeast of Grand Isle, Louisiana, 27°11.43′N; 90°01.37′W) and examined for parasites in synergy with other research activities on 31 July 2013. Yellowfin tuna were morphologically identified in the field by having 26–34 total gill rakers on the first gill arch, elongate dorsal and anal rays that exceed 20% of fork length, and ventral surface of liver without prominent striations and having a central lobe slightly longer than left and right lobes [18].

The gill, buccal cavity, and external body surfaces of the infected yellowfin tunas were carefully examined with the naked eye and photographed in the field. Select monogenoids intended for taxonomy were removed alive from the fish using fine forceps, heat-killed with freshwater heated to 60 °C, and immediately fixed in 10% neutral buffered formalin. Later, whole, formalin-fixed specimens were transferred to and held in a vial of 5% neutral buffered formalin, placed overnight in distilled water, stained overnight in Van Cleave's hematoxylin with several additional drops of Ehrlich's hematoxylin, made basic in 70% ethanol with lithium carbonate and butyl-amine, dehydrated, cleared in clove oil, permanently mounted on over-sized glass slides using Canada balsam [19,20], and studied using a compound microscope with differential interference contrast (DIC) optics. The 5 specimens and selected samples of lesioned skin for scanning electron microscopy (SEM) were washed in de-ionized water, dehydrated through a graded ethanol series, critical point dried in liquid CO_2, mounted on standard aluminum SEM pin stubs with double-sided carbon tape, sputter-coated with gold palladium (19.32 g/cm^3; 25 mA), and viewed with a Zeiss EVO 50VP scanning electron microscope. Illustrations of stained, whole-mounted specimens were made with the aid of a Leica DM-2500 equipped with differential interference contrast (DIC) optical components and a drawing tube. Photographs of whole-mounted specimens were made on that microscope using a digital single lens reflex camera. Parasite measurements are herein reported in micrometers (μm), followed by their mean and number measured in parentheses. Measurements of monogenoid specimens are reported as a range followed by, in parentheses, the mean and number of specimens measured (n). For comparative purposes, and because it was an outlier, values for the indicated feature of the smallest collected specimen are reported in brackets.

The specimen for molecular biology was removed alive from an infected fish using fine forceps, immediately preserved in a vial of 95% EtOH and stored at −20 °C. Total genomic DNA from that specimen was extracted using a DNeasy™ Blood and Tissue Kit (Qiagen) according to the manufacturer's instructions, except for the final elution step wherein only 100 μl of elution buffer was used, in order to increase the final DNA concentration in the eluate. DNA concentrations of samples were quantified (i.e., ng/μl) using a NanoDrop spectrophotometer (Thermo Fisher Scientific, Waltham, MA). Polymerase chain reaction (PCR) amplifications of the large subunit ribosomal DNA (28S) was performed in a total volume of 50 μl, consisting of approximately 2.5 μl of template DNA, 10 μl of 5× TAQ Buffer, 1 μl of DNTPs (Promega, Madison, WI), 1 μl of the forward primer "C1" (5′-ACC CGC TGA ATT AAG CAT-3′) [21], and 1 μl of the reverse primer "D2" (5′-TGG TCC GTG TTT CAA GAC-3′) [21], 0.3 μl of TAQ polymerase (5 Primer Inc., Gaithersburg, MD) and 34.5 μl of molecular grade water. The PCR amplification profile comprised an initial 5 min at 94 °C for denaturation, followed by 29 repeating cycles of 94 °C for 1 min for denaturation, 56 °C for 1 min for annealing, and 72 °C for 1 min for extension, followed by a final 10 min at 72 °C for extension. PCR products were viewed on a 1% agarose gel stained with ethidium bromide. Sequencing was performed by Lucigen Corporation (Madison, WI) using the same primers as were used in the PCR. Sequence assembling and analysis of chromatograms was conducted using BioNumerics version 7.0 (Applied Maths, Sint-Martens-Latem, Belgium).

The partial 28S rDNA sequence data generated during this study was aligned with those for capsalines available on GenBank.

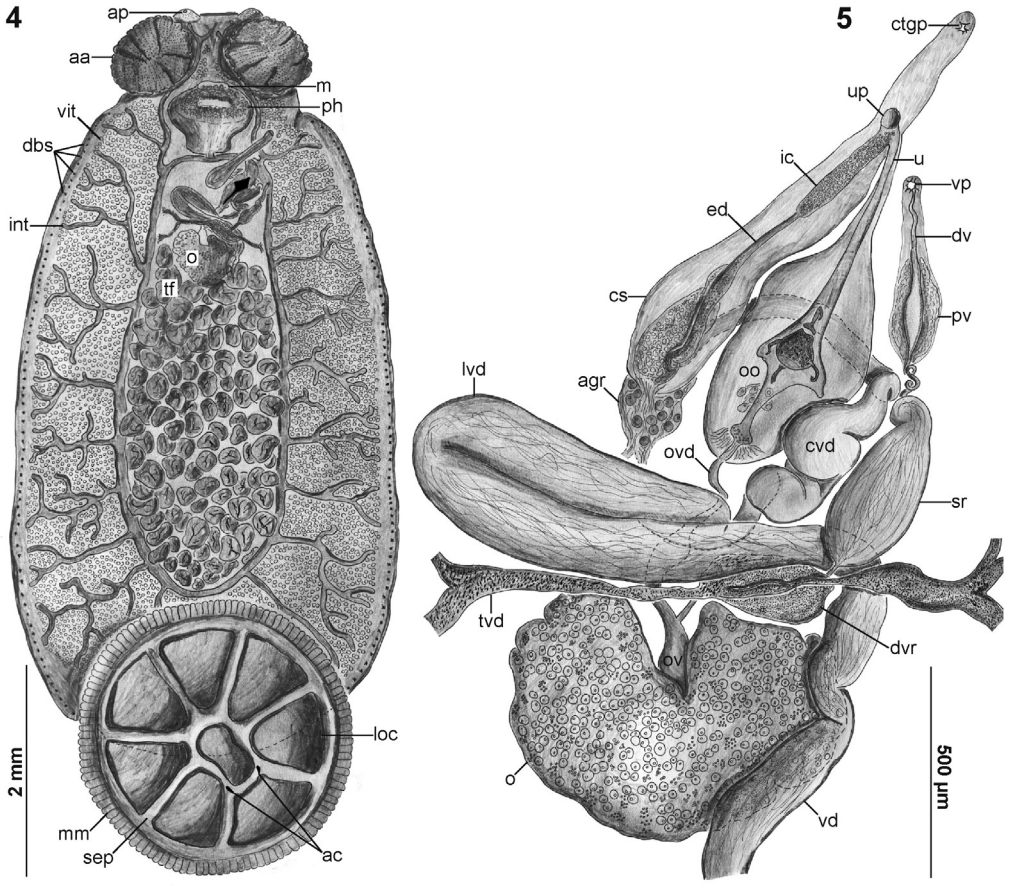

Figs. 4–5. *Capsala* cf. *biparasiticum* (Goto, 1894) Price, 1938 (Monogenoidea: Capsalidae) from epithelium of inner surface of the operculum of yellowfin tuna, *Thunnus albacares* (Perciformes: Scombridae) captured in the north-central Gulf of Mexico's outer continental shelf. Scale bar value aside each bar. (4) Body of adult specimen showing dextral anterior pore (ap), anterior attachment organ (aa), mouth (m), pharynx (ph), vitellarium (vit), dorsolateral body sclerites (dbs), intestine (int), ovary (o), testicular field (tf), marginal membrane (mm) of haptor, septum (sep), accessory sclerite (ac), and loculus (loc). (5) Genitalia showing common terminal genital pore (ctgp), uterine pore (up), uterus (u), inverted cirrus (ic), vaginal pore (vp), ejaculatory duct (ed), distal vagina (dv), proximal vagina (pv), cirrus sac (cs), ootype (oo), accessory gland reservoir (agr), ovo-vitelline duct (ovd), coiled ascending portion of vas deferens (cvd), oviduct (ov), seminal receptacle (sr), loop of vas deferens (lvd), dorsal vitelline reservoir (dvr), transverse vitelline duct (tvd), ovary (o), and vas deferens (vd).

Homologous sequences from the capsalid species *Allobenedenia epinepheli* (GenBank EU707801), *Benedenia lutjani* (AY033939), *Benedenia rohdei* (AY033940), and *Neobenedenia melleni* (JN797596) were used as outgroups (sensu [22]). The ingroup comprised a representative of the newly collected specimens (KT445886), *Capsala laevis* (JN980396), *Capsala martinieri* (AF382053), *Capsala pricei* (JN980397), *Capsala* sp. (EF653379), *Capsaloides cristatus* (JN711434), *Capsaloides* sp. (JN711435), *Entobdella australis* (AY486153), and *Entobdella hippoglossi* (AY486151). Sequences were aligned using MAFFT [23] with default settings implemented in the CIPRES Science Gateway V. 3.3 [24]. The resulting alignment was refined by eye using MEGA version 5.2.2 [25] and ends of each fragment were trimmed to match the shortest sequence. Ambiguous positions were identified and removed using the Gblocks server [26] with settings for a more stringent selection. Model of evolution for the Bayesian inference (BI) and Maximum Likelihood (ML) analyses was selected based on the Akaike Information Criterion [27] as implemented in the jModelTest version 2.1.4 [28,29]. The GTR + I + G (proportion of invariable sites = 0.442 and gamma distribution = 3.161) model was inferred as the best estimator. BI was performed using the Metropolis-coupled Markov chain Monte Carlo method (MC^3) in MrBayes version 3.2.3 [30–32] and run on CIPRES [24] according to the following parameters: nst = 6, rates = invgamma, ngammacat = 4, and default priors. Analyses were run in duplicate each containing four independent chains (three heated and one cold chain) (nchains = 4) for 1.0×10^7 generations (ngen = 10,000,000) sampled at intervals of 1000 generations (samplefreq = 1000). Results of the first 2000 sampled trees were discarded as "burn-in" based on the stationarity of the likelihood values, assessed by plotting the log-likelihood values of the sample points against generation time using Tracer version 1.5 [33]. All retained trees were used to estimate posterior probability of each node. A majority rule consensus tree with average branch lengths was constructed for the remaining trees using 'summarize the trees' (sumt) in MrBayes. Resulting phylogenetic trees were visualized using FigTree v1.3.1 [34]. ML phylogenetic analyses were conducted in MEGA 5. Bootstrap values were estimated from 10,000 replicates. Branch support for BI and ML analyses were considered as significant when posterior probabilities were >0.95 and bootstrap values were >70%, respectively.

Areas of lesioned skin intended for histopathology were excised and immediately preserved in 10% neutral buffered formalin in the field. In the laboratory, fixed tissue samples were grossed such that the region of the black halo (Figs. 1–3) surrounding each attached parasite was centered. Each histopathology sample then was dehydrated in a graded series of EtOHs, embedded in paraffin, sectioned at 4 μm, routinely stained with hematoxylin and eosin, mounted on glass slides, and photographed on the compound microscope.

Fish scientific names, taxonomic authorities, and dates for fish taxa follow Eschmeyer [35] and Eschmeyer and Fong [36]. Higher-level fish classification and nomenclature follows Nelson [37] and Collette [18]. Classification and anatomical terms for the parasites were informed by Chisholm and Whittington [7,38]. Regarding parasite nomenclature, both "*biparasiticum*" and "*biparasitica*" appear in the taxonomic

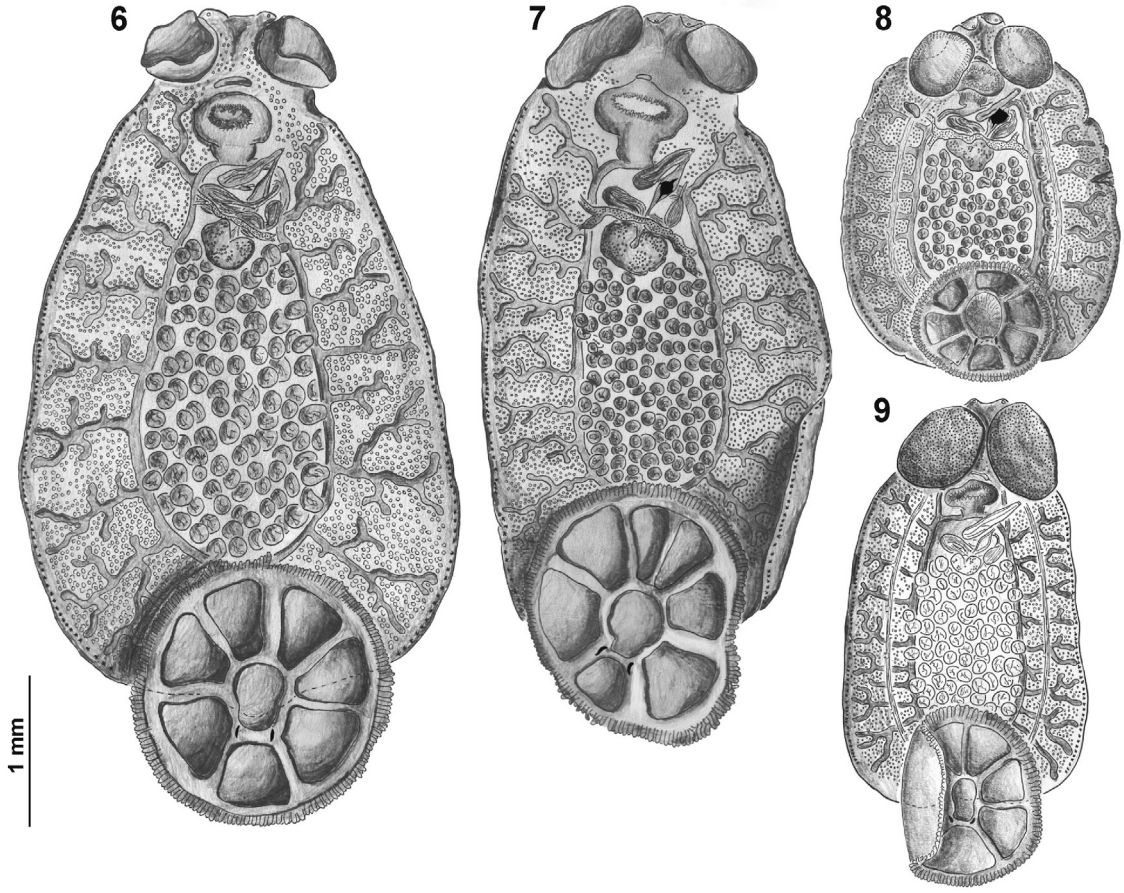

Figs. 6–9. Capsalines from yellowfin tuna, *Thunnus albacares* (Perciformes: Scombridae) and parasitic copepods infecting yellowfin tuna, ventral view, all same scale. (6) Holotype (USNP Coll. No. 63596 974-22) of *Capsala neothunni* Yamaguti, 1968 from yellowfin tuna, *Thunnus albacares* (syn. *Neothunnus macropterus*) in the central Pacific Ocean off Hawaii, USA. (7) Voucher (BMNH Coll. No. 1975.9.17.11) of *Capsala abidjani* (Bussiéras and Baudin-Laurencin, 1970) Chisholm and Whittington, 2007 (syn. *Caballerocotyla abidjani*) from buccal cavity of yellowfin tuna off South Africa. (8) Voucher (HWML Coll. No. 44308) of *Capsala biparasiticum* (Goto, 1894) Price, 1939 (as *C. biparasiticum*) from dorsum of parasitic copepod (*Elytrophora* sp.) collected from the "gills" of yellowfin tuna from off Christmas Island (Line Islands) in the south-central Pacific Ocean. (9) Voucher (USNM Coll. No. 1283169) of *Capsala* cf. *biparasiticum* (Goto, 1894) Price, 1939 from the inner surface of the operculum of yellowfin tuna captured in the north-central Gulf of Mexico's outer continental shelf (27°11.43′N; 90°01.37′W).

literature. Article 30.2.4. of the International Code of Zoological Nomenclature [39] states that, "*If no gender was specified or indicated, the name is to be treated as masculine, except that, if the name ends in -a the gender is feminine, and if it ends in -um, -on, or -u the gender is neuter.*" As such, the neuter "*biparasiticum*" should be retained as in "*C. biparasiticum*," not "*biparasitica*" as per authors following Price [9].

3. Results

3.1. Taxonomy (Figs. 4–21)

Morphological diagnosis based on 10 stained, whole-mounted voucher specimens (USNM Nos. 1283167–69), 4 sectioned specimens, and 5 sputter-coated specimens from the inner surface of the operculum of 2 yellowfin tuna, T. albacares (measurements of smallest specimen in brackets) in the northern GOM off Louisiana: Body transparent or opaque in life with dark areas in living specimens comprising vitellarium, pyriform, having smooth-surfaced and equally-rounded lateral edges lacking scalloped margins, 7300–10,240 (8351; 9) [2760] long excluding haptor, 3600–5880 (4613; 9) [1660] in maximum width or 1.42–2.18 [1.66] × longer than wide, with 2 pairs of eyespots approximately dorsal to mouth, body surface papillae not evident with light microscopy dorsally and ventrally, with a sudden diminution of breadth in anterior part immediately behind anterior suckers (Figs. 4 and 9). Anterior attachment organs bilaterally symmetrical, slightly wider than long but approximately 680–1000 (816; 9) [680] in diameter or 8–12% (10%; 9) [21%] of body width, connecting with body in center of attachment organ, strongly ventrally concave, bearing numerous ventral papillae; ventral papillae of anterior attachment organ distributing primarily lateral to strongly concave central portion of sucker (Figs. 4, 9, 15). Anterior body end having a pair of anterior pores each opening atop a tegumental mound (Figs. 4, 9, 15, 16), likely associated with adhesion, seemingly exuding a substance in some SEM specimens (Fig. 16); each anterior pore approximately 20–30 (24; 9) [10] wide; tegumental mound approximately 125–225 (165; 9) [75] wide at base (Fig. 16). Haptor typical of *Capsala* spp. (Figs. 4, 6–9), circular, 2540–3220 (2880; 9) [1080] long (excluding marginal membrane) or 49–84% [65%] of maximum body width, extending beyond posterior body margin 1080–1560 (1422; 9) [580] or 15–21% (17%; 9) [21%] of body length, having 4 anterior loculi, 3 posterior loculi, and 1 keyhole-shaped central loculus, having marginal membrane, with ventral papillae covering ventral surface of loculi, including 1 pair of accessory sclerites (Figs. 4, 9), deeply imprinting skin (Fig. 17) and affecting adjacent skin at attachment site (Fig. 18). Haptoral marginal membrane scalloped, highly muscular, with neighboring scallops functioning as a sphincter or sucker, comprising a series of overlapping lamellar extensions of haptoral tegument that likely form a contiguous gasket, of approximately uniform width around haptor rim, 160–280 (202; 9) [80] wide, having approximately 108–140 (126; 9) [123] scallops total; each scallop approximately 70–200 (99; 9) [30] wide (Figs. 4, 9), markedly imprinting the skin (Fig. 17). Haptoral septa narrow, none bifid where connecting to haptoral rim. Accessory sclerites typical for that of *Capsala* spp., difficult

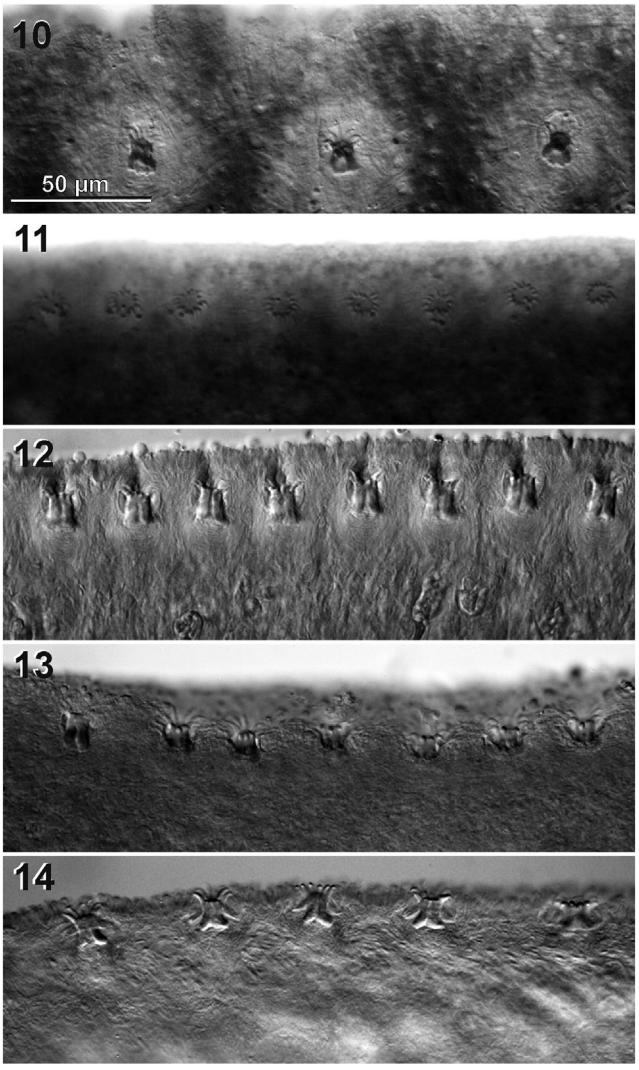

Figs. 10–14. Light micrographs (differential interference contrast) showing distributions and relative sizes of dorsomarginal body sclerites (dextral portion of body margin immediately posterior to anterior sucker); scale bar applies to all figures. (10) *Capsala* cf. *biparasiticum* (present study; USNM 1283167), large adult specimen. (11) *Capsala* cf. *biparasiticum* (present study; USNM 1283169), smallest adult specimen. (12) *Capsala biparasiticum* (HWML Coll. No. 44308). (13) *Capsala neothunni* (USNP Coll. No. 63596 974-22). (14) *Capsala abidjani* (BMNH Coll. No. 1975.9.17.11).

to assess due to dorso-ventral orientation within muscular haptor (i.e., sclerites slanting towards host surface), each having sharp exposed point directing anteriad, slightly bent laterad, approximately equal in total length and thickness, 60–110 (81; 7) long or 2–4% (3%; 6) of haptor diameter, 10–15 (12; 8) thick, protruding from haptor ventral surface at posterior corners of keyhole-shaped central loculus; marginal hooklets not evident. Equally-spaced dorsomarginal body sclerites distributing in even dextral and sinistral columns extending most of body length, approximately 25–75 (52; 9) [20] from body margin (Figs. 10, 11); dorsomarginal sclerites each residing within a tegumental pocket; dextral column having a total of 65–81 (73; 9) [58] sclerites each having many cusps and each 13–20 (16; 9) [10] wide at base inserting into tegument, extending posteriad and terminating anterior to haptoral margin; body margin lacking dorsomarginal body sclerites for 375–560 (467; 9) [160] or 4–7% (6%; 9) [6%] of body length immediately posterior to anterior attachment organ. Mouth medial, opening between anterior attachment organs (Figs. 4, 9, 15). Pharynx 700–980 (804; 9) [480] long, 860–1240 (1024; 9) [520] wide, extensively papillate about pharynx rim, connecting posteromedially with esophagus; papillae of pharynx approximately 45–75 (63; 9) long, 25–55 (44; 9) wide at base (Figs. 4, 9). Intestine thin-walled with dendritic extensions running laterad and mediad for length of main branches of intestine (Figs. 4, 9). Nerve system similar to that of *Capsala* spp. (see Barse and Bullard [20]). Excretory pores (not illustrated) lateral, immediately posterior to anterior attachment organs.

Testes densely packed in a single layer between main cecae and extending slightly lateral to cecae, numbering approximately 96–106 (100; 6) [approximately 70], slightly lobed or not lobed, 200–360 (249; 9) [80] in diameter; testicular field terminating approximately 1160–1580 (1378; 9) [440] from lateral body margin and 1880 or 26% of body length from posterior end of body, 3160–4900 (3767; 9) [1100] long or 40–54% [40%] of body length, 1140–2800 (1842; 9) [760] wide or 13–30% (22%; 9) [46%] of body width, extending to level of anterior margin of ovary, extending posteriad to near anterior margin of haptor, coextensive with intestine, nerve, and vitelline ducts (Figs. 4, 9). Putative glands of Goto distributing among testes (not illustrated), each approximately 55–110 (71; 8) [20] in diameter, including 2–4 spheroid bodies within a seemingly transparent, slightly eosinophilic capsule. Vasa efferentia ventral to testicular field, extensively branched, collecting anteriorly and forming common duct overlapping sinistral portion of ovary. Vas deferens coalescing ventral to testicular field and extending anteriad, sinistral and slightly ventral to ovary, curving mediad dorsal to transverse vitelline duct and vitelline reservoir before crossing midline to form a marked dextral loop 560–1240 (840; 9) [260] long or 16–21% (18%; 9) [16%] of body width and 120–240 (173; 9) [60] in maximum width, crossing midline again and turning anteriad to form ascending vas deferens (Figs, 4, 5, 9); ascending vas deferens comprising an extensively convoluted proximal portion and relatively straight distal portion that connects to cirrus sac (Fig. 5); proximal portion of ascending vas deferens extending anteriad 425–600 (494; 9) [300], with 3–7 (5; 9) [3] coils; distal portion of ascending vas deferens straight, arching dorsal to uterus, extending mediad approximately 300–550 (414; 9) [150] before connecting with proximal portion of cirrus sac (Fig. 5). Cirrus sac 960–1400 (1111; 9) [420] long or 17–30% (25%; 9) [25%] of body width, 100–240 (156; 9) [60] in maximum width, enveloping male accessory gland reservoir, ejaculatory duct, and inverted cirrus; male accessory gland reservoir occupying proximal portion of cirrus sac, kidney-bean shaped (strongly bi-lobed or not) if cirrus inverted, 165–350 (252; 9) [105] long or 14–31% (21%; 8) [25%] of cirrus sac length, 90–130 (113; 8) [50] in maximum width (Fig. 5); cirrus papillae each approximately 5–10 (6; 7) wide. Ejaculatory duct connecting accessory gland reservoir and cirrus, 125–325 (252; 9) [100] long or 11–30% (16%; 9) [24%] of cirrus sac length. Inverted cirrus length 230–315 (271; 7) [200] long or approximately 20% of cirrus sac length (Fig. 5). Common terminal genital pore ventral, sinistral, opening immediately posterior to anterior attachment organ and lateral to pharynx, 1060–1580 (1267; 9) [680] or 13–17% (15%; 9) [25%] of body length from anterior body end, approximately 150 or 2% of body length posterior to anterior attachment organ (Fig. 5).

Ovary medial, typically having 2 anteriad lobes flanking germarium, immediately posterior to transverse loop of vas deferens and transverse vitelline duct, 540–820 (647; 9) [120] long or 6–10% (8%; 9) [4%] of body length, 580–920 (776; 9) [180] wide or 16–22% (17%; 9) [11%] of body width or 0.63–1.0 (0.85; 9) [0.67] × longer than wide, enclosing a germarium 130–210 (163; 5) [50] long and 125–225 (170; 5) [60] wide, more or less distinctive depending on staining attributes of specimen (Fig. 5). Oviduct extending anteriad 150–550 (399; 9) [160] from medial portion of ovary comprising germarium, 15–75 (52; 9) [25] in maximum width, dorsal to transverse vitelline duct and dextral loop of vas deferens. Vitellarium typical of species of *Capsala* (see Barse and Bullard, 2013) (Figs. 4–9), having follicles and collecting ducts that coalesce and form transverse vitelline duct plus vitelline reservoir; vitelline follicles each 40–60 (48; 9) in diameter, extending laterad to 125–225 (159; 9) from body margin (Figs. 4, 9). Transverse vitelline duct extending 740–1560 (1082; 9) across width of body, 60–180 (98; 9) in maximum width (Fig. 5); vitelline reservoir sinistral, a distinct chamber not

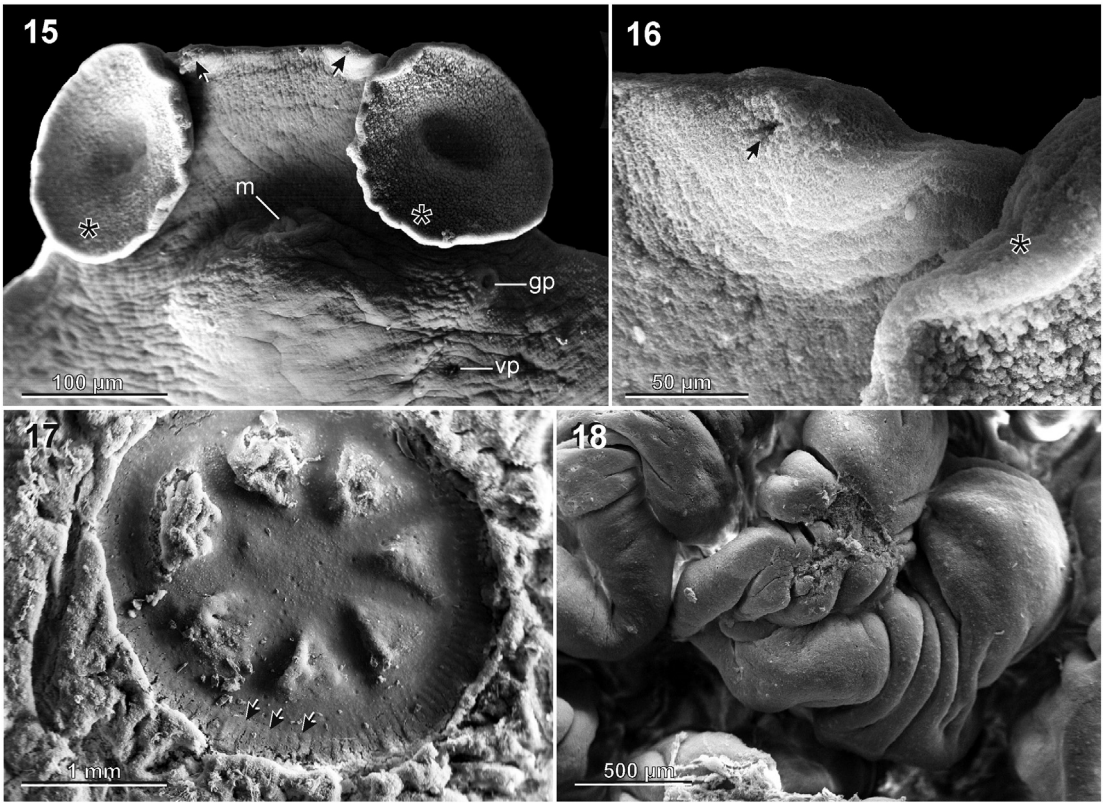

Figs. 15–18. Scanning electron micrographs of *Capsala* cf. *biparasiticum* (Goto, 1894) Price, 1938 (Monogenoidea: Capsalidae) from epithelium of the inner surface of the operculum (immediately ventral to opercular pseudobranch) of yellowfin tuna, *Thunnus albacares* (Perciformes: Scombridae) captured in the north-central Gulf of Mexico's outer continental shelf. Scale bar value aside each bar. (15) Anterior end of body showing densely papillate ventral surface of the disc-shaped anterior attachment organs (*), mouth (m), common terminal genital pore (gp), vaginal pore (vp), and head pores (arrows), which are terminal and appear slightly medial to the inner margin of each anterior attachment organ. (16) Higher magnification view of the sinistral head pore showing its opening (arrow) medial to the anterior attachment organ (*). (17) Imprinted epidermis and dermis indicating the haptoral attachment site of *C.* cf. *biparasiticum*. Note that gaps between the pie-shaped features comprise the impression left by the radially arranged haptoral septa. Peripherally, an impression of the haptoral marginal membrane is evident (arrows). The impression of the keyhole-shaped central loculus is evident left of center. (18) High magnification view of rugose epidermis in the area immediately adjacent to attachment sites of adult specimens of *C.* cf. *biparasiticum*.

a simple expansion of transverse vitelline duct, variable in size depending on volume of vitelline material it contains, 120–240 (175; 8) in diameter, dorsal to transverse vitelline duct and dextral loop of vas deferens (Fig. 5). Vaginal pore sinistral, posterior to level of esophagus and male genital pore, 1320–2000 (1620; 9) [780] or 18–21% (19%; 9) [28%] of body length from anterior end (Fig. 5). Vagina comprising

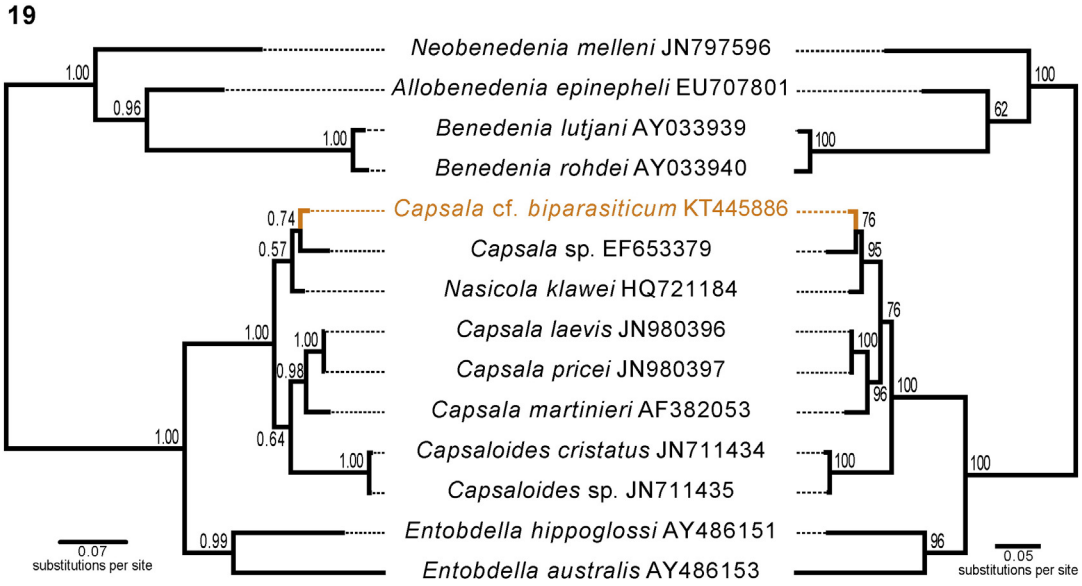

Fig. 19. Phylogenetic relationships of capsalids reconstructed by Bayesian inference (left) and Maximum Likelihood (right) and based on partial D1–D2 domains of 28S from 14 taxa (majority rules consensus tree and best tree, respectively). Numbers aside tree nodes indicate posterior probability (Bayesian inference, left) and bootstrap values (Maximum Likelihood, right).

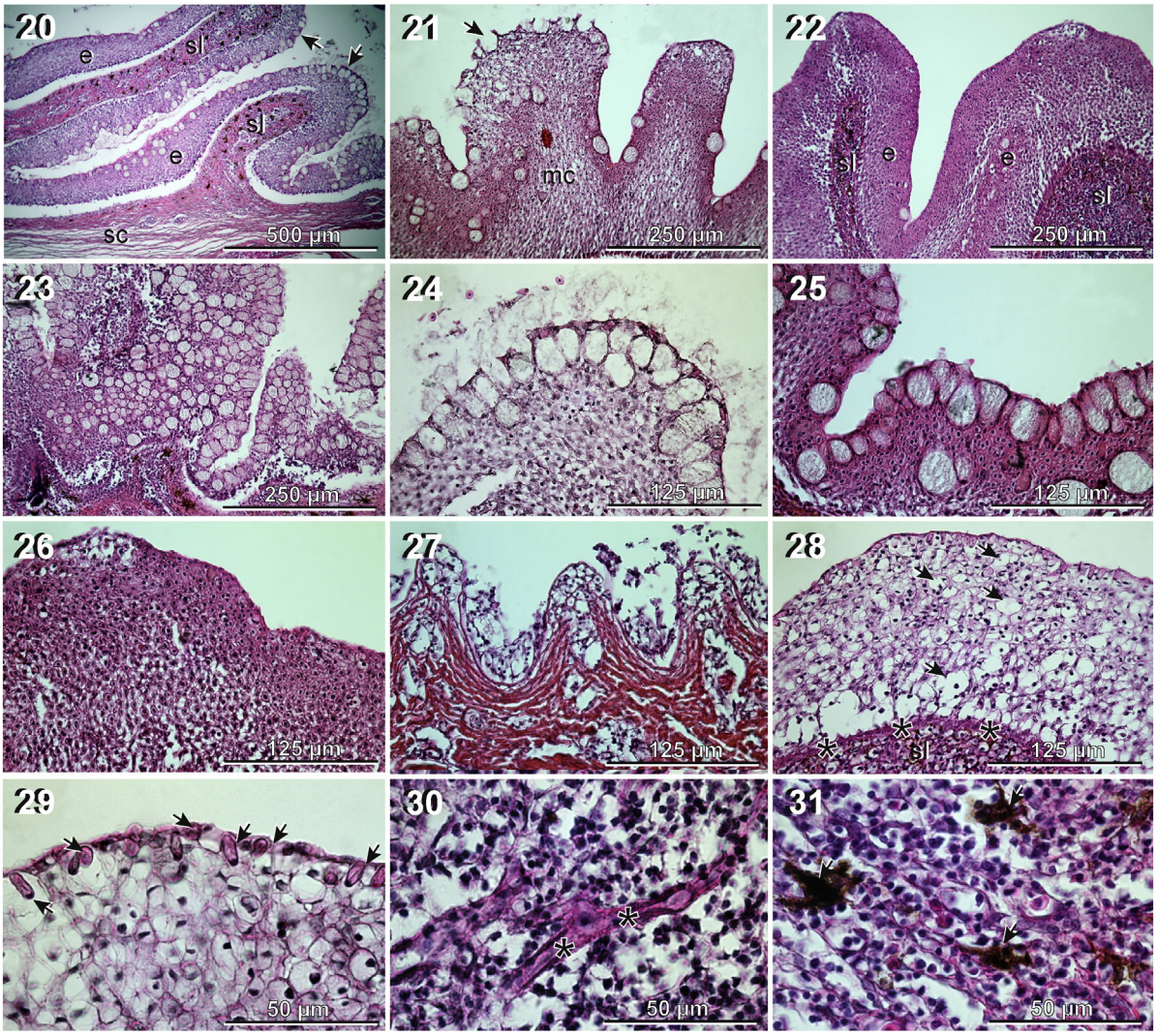

Figs. 20–31. Histological micrographs (hematoxylin and eosin, 4-micrometer sections) of infection sites of *Capsala* cf. *biparasiticum* (Goto, 1894) Price, 1938 (Monogenoidea: Capsalidae) from epithelium of the inner surface of the operculum of yellowfin tuna, *Thunnus albacares* (Perciformes: Scombridae) captured in the north-central Gulf of Mexico's outer continental shelf. Scale bar value aside each bar. (20) Hyperplastic epidermis (e), stratum laxum (sl), and stratum compactum (sc) in infection site of *C.* cf. *biparasiticum* showing extensive folding (rugosity) of skin, abundant apical goblet cells (arrows), and melanin (black splotches) in the stratum laxum. (21) Epidermis, appearing moderately columnar, showing mass of proliferated malpighian cells (mc) and goblet cells that are intact or ruptured (arrow) on epidermal surface. (22) Epidermis, appearing moderately columnar, showing extensive epidermal hyperplasia with few goblet cells in vicinity of haptoral attachment site of *C.* cf. *biparasiticum*. (23) Extensive involvement of goblet cells in epidermis adjacent to the haptoral attachment site of *C.* cf. *biparasiticum*. (24) Apical goblet cells in the vicinity of the tissue in Fig. 24 showing the putative release of mucus precursor over surface of skin. (25) Margination of goblet cells in infection site. (26) Mound-like appearance of proliferated (hyperplastic) malpighian cells near attachment site of *C.* cf. *biparasiticum*. (27) Systolic, wave-like, appearance of stratum compactum underlying a seemingly obliterated (although perhaps artifactitious) epidermis wherein cell-to-cell adhesions were weak or broken. (28) Epidermis showing apparent hydropic degeneration (water logging) of malpighian cells (arrows), disassociation of stratum germinativum (*) from stratum laxum (sl), and interspersed rodlet cells in epidermis. (29) Higher magnification view of the area of infected tissue shown in Fig. 28 showing rodlet cells (arrows) in apical layer of epidermis. (30) Extensive involvement of lymphocytic infiltrates (most of the cells in the field of view) and blood vessels (*) associated with the stratum laxum immediately beneath haptoral attachment site of *C.* cf. *biparasiticum*. (31) Melanin-like granules (arrows) associated with stratum laxum immediately beneath haptoral attachment site of *C.* cf. *biparasiticum*.

distal and proximal portions that extend directly posteriad from vaginal pore 410–705 (516; 9) [170] plus a seminal receptacle (Fig. 5). Distal vagina a thin tube extending directly posteriad from vaginal pore; proximal vagina a laterally expanded and more glandular tube. Seminal receptacle marked by an anterior constriction and tightly coiled segment of the duct, 240–420 (354; 9) [160] or 51–95% (80%; 5) [47%] of vagina total length, 115–200 (168; 9) [80] in maximum width, narrowing posteriorly before connecting with vitelline reservoir (Fig. 5). Ootype 400–625 (523; 8) [120] long, 255–445 (331; 8) [80] wide, occupying space between cirrus sac and tightly coiled ascending portion of vas deferens, ventral to distal portion of ascending vas deferens; uterus a simple, short tube extending 10–50 (25; 3) anteriad from ootype and opening within common atrium accommodating terminal male genitalia (Fig. 5).

3.2. Taxonomic summary

Type host for Capsala biparasiticum: parasitic copepod "probably of the genus *Parapetalus*" infecting the "gill" of yellowfin tuna (Goto, 1894).

Type locality: Northwest Pacific Ocean (host of the type host landed at Misaki, Japan seaport); *other localities*: see Table 1.

Site of infection and other host species: Table 1.

Prevalence and intensity of infection: 2 of 19 (0.11) yellowfin tuna were infected with 36 and 27 specimens of *C.* cf. *biparasiticum*.

3.3. Molecular diagnosis (Fig. 19)

The data matrix used for Bayesian inference (BI) and Maximum Likelihood (ML) analyses comprised 568 positions per taxon (302

conserved, 266 variable, and 213 parsimony informative) (Fig. 19). Topologies recovered by both methods were similar. In both analyses, *C.* cf. *biparasiticum* and *Capsala* sp. (EF653379 of Aiken et al. [1]) grouped as sister taxa. Oddly, that clade showed a strong phylogenetic affinity to the 28S sequence for a specimen of *Nasicola klawei* (HQ721184 of Bullard et al. [40]) collected from the nose of GOM yellowfin tuna (Fig. 19). The resulting trees also showed some discrepancies: in the tree derived from BI, the clade comprising (*N. klawei* (*C.* cf. *biparasiticum*, *Capsala* sp.)) is sister to *Capsaloides* + *Capsala*, whereas the ML tree shows *Capsaloides* as a sister taxon to the clade formed by (*N. klawei* (*C.* cf. *biparasiticum*, *Capsala* sp.)) + *Capsala*. Moreover, ML analysis yielded a tree with higher nodal support values than those recovered in the BI analysis (Fig. 19). Changing parameters (more relaxed GBLOCK settings) for exclusion of ambiguous positions in the alignment affected placement of *N. klawei*, *C.* cf. *biparasiticum*, and *Capsala* sp. in the resulting optimal topologies (data not shown). That, coupled with the low nodal support depicted for those taxa in both analyses (Fig. 19), suggested that denser taxon sampling and additional sequence data may significantly improve the resolution of this phylogeny. A short (367 bp) 28S sequence for *Capsala onchidiocotyle* (AF131712; from *Thunnus thynnus*) differed by 6 bps with the sequence of *C.* cf. *biparasiticum* (1.6%), and these taxa grouped in separate clades in all analyses that included just short sequences (i.e., ~400 bp) (data not shown). The short 28S sequences of Perkins et al. (2009) for *C. pricei* and *C. laevis* are 100% identical, and the 870 bp-length 28S sequences for those taxa deposited by Yang and Yang and Hu, respectively, in 2011 (unpublished), differ by only 5 bps. Those differences are principally concentrated on 5′ end of the sequences; perhaps resulting from erroneous base calls.

3.4. Pathology (Figs. 1–3; 17–18, 20–31)

3.4.1. Gross observations of lesion (Figs. 1–3)

Adult capsalines (intensities = 27 and 36) were attached to the inner surface of the sinistral and dextral opercula of 2 of 11 (prevalence = 0.18) yellowfin tuna (53–128 cm fork length). A detailed search of other regions of the body surface failed to reveal an additional specimen, and no ectoparasitic copepod was observed on either capsalid-infected yellowfin tuna. Capsalines were distributed in the posterior half (excurrent portion) of each operculum, with most specimens attaching to the inner surface of the operculum immediately below the opercular pseudobranch (Fig. 1).

The haptoral attachment site of adult capsalines was located within a whitish crater-like depression (1–1.5 cm in diameter) surrounded by a blackish halo of extensively rugose skin (Figs. 1–3). Nearly transparent adult capsalines resided within the center of each blackish halo (Figs. 2 [*in vivo*], 3 [post-fixation]). Less obvious alterations to skin became evident upon inspection with the stereo-dissecting microscope and comprised pockmarked-like, irregularly-shaped oblong or semicircular epidermal pits (Fig. 2) dispersed between and among the crater-like capsalid attachment sites. Each infected yellow tuna operculum had 4–8 of these blackish halo-shaped features (Figs. 1–3), which were obviously visible upon reflection of the operculum anterodorsad. Additional capsalid specimens were attached between and among these blackish halo-like foci and the trailing edge of the operculum but those capsalid specimens were not associated with a grossly discolored lesion. Some capsalines evidently became detached upon tissue fixation and processing in the laboratory but haptoral attachment sites were clearly marked by the circular impressions of the septate haptor (Figs. 3, 17).

3.4.2. Scanning electron microscopy of lesion (Figs. 17, 18)

The haptor of the adult capsalines was tightly adhered to the apical surface of the epidermis and capable of imprinting the tissue. The periphery of the haptoral attachment site shows the impression of the scallops comprising the haptoral marginal membrane (Fig. 17). The epidermis immediately beneath the haptor was smooth (compacted); whereas, the areas of epidermis immediately adjacent to the haptoral attachment site were uneven and rugose. Extending out from the site of haptoral attachment, the skin appeared to become progressively more folded, rugose (Fig. 18). No evidence of adhered bacterial cells was observed and no erythrocyte was associated with the skin of examined samples.

3.4.3. Histopathology of lesion (Figs. 20–31)

Infected skin exhibited many of the typical pathological changes associated with ectoparasitic infections of marine fishes but the changes we observed in these infections seemed severe. In the tissues we subsampled for histopathology and in sites nearby attached capsalid specimens, we did not detect any area comprising normal fish epidermis, i.e., a flat and even, thin, single or several cell-thick layer of malpighian cells overlying a dermis lacking lymphocytic infiltrates, rodlet cells, and eosinophilic granulocytes. As indicated by stereomicroscopy and SEM, infected skin was highly folded and scaffolded by extensive folding of the stratum laxum of the dermis (Figs. 20–22). The epidermis covering these rugose areas of skin was markedly thickened, comprising a dense layer of malpighian cells (Figs. 25, 26) and containing abundant goblet cells (intact or ruptured) at the apical surface of the epidermis (Figs. 20, 21, 23–25). In some foci of infection, the skin was so extensively altered or folded that it appeared columnar (Figs. 18, 21) or mounded (Fig. 22) in section. The epidermis typically was intact but showed signs of weakened or compromised cell-to-cell adhesions that were marked by apparent sloughing or putatively artifactitious loss of epidermis during tissue processing (Fig. 27). The probable epithelial hyperplasia evident near haptoral attachment sites formed a markedly thickened layer that was 200–500 μm thick (Figs. 25, 26). In some instances malpighian cells were seemingly intact (having an eosinophilic cytoplasm without vacuolization; Fig. 25) and in other instances they appeared to exhibit hydropic degeneration (water logging) and necrosis (Figs. 27–29). In some instances the stratum germinativum was seemingly loosely associated with the stratum laxum of the dermis (Fig. 28). Goblet cells were abundant in the epidermis (Figs. 23–25), and in some foci they were clearly observed in sections to be lysing and releasing cytoplasmic contents over the surface of the skin (Fig. 24). In some instances we conservatively estimated that 75% of the epidermis comprised goblet cells (Fig. 23). These goblet cells formed multilayered columns or contiguous rows of cells that dominated the epidermis about the attachment sites of adult capsalines. Goblet cells were lacking in some areas of putatively extensive epidermal hyperplasia (Fig. 26). Rodlet cells were moderately abundant in the lesioned epidermis and were interspersed between goblet cells or formed a discontinuous layer of cells along the apical surface of the epidermis (Fig. 29). The dermis beneath and adjacent to attached specimens of the capsaline was extensively altered. We noted extensive lymphocytic infiltrates that comprised the majority cell type in some areas (Figs. 30, 31), and, in these zones, we detected evidence of vascularization, although perhaps unrelated to infection (Fig. 30). Melanin was abundant as indicated by the gross appearance of the lesions (Figs. 20, 30, 31). No evidence suggestive of a fungal, viral, or bacterial pathogen was detected in any histological section.

4. Discussion

4.1. Diagnosis of capsalines infecting yellowfin tuna

Chisholm and Whittington [7], based on features that are intuitively not vulnerable to fixation artifact or specimen preparation, synonymized 24 of 60 named capsalines; several of which were based on incomplete or inadequate original descriptions or that lacked extant type material(s). Informed by that work, published infection records for yellowfin tuna comprise *C. biparasiticum* (Goto, 1894) Price, 1938; *Capsala neothunni* (Yamaguti, 1968) (jr. subj. syn. *C. biparasiticum*);

Capsala abidjani (Bussieras and Baudin-Laurencin, 1970) (as *Caballerocotyla abidjani*; jr. subj. syn. *C. biparasiticum*); and *Capsala verrucosa* Bussieras, 1972 (jr. subj. syn. *Capsala paucispinosa*). Those synonymies plus that of *Caballerocotyla* with *Capsala* result in 2 accepted species of *Capsala* that infect gill and/or buccal cavity of yellowfin tuna: *C. biparasiticum* from the Pacific Ocean [8,11,41] and eastern Atlantic Ocean [15,42] plus *C. paucispinosa* from the eastern Atlantic Ocean. Neither species has been reported from a species of *Thunnus* in the GOM or northwestern Atlantic Ocean.

We identified our specimens as *C.* cf. *biparasiticum* because they were morphologically indistinguishable from the description provided by Goto [8], they resembled museum specimens regarded as junior subjective synonyms of *C. biparasiticum*, and they keyed to *C. biparasiticum* as per Chisholm and Whittington [7]. We also added some features previously not ascribed to Capsalinae (e.g., anterior pores) or to *C. biparasiticum* (see description above). However, we remain uncertain of the species identity of this capsaline because (i) no type material exists for *C. biparasiticum*, (ii) Goto's [8] description is not restrictive, and (iii) no specimen has been collected from the type host (a parasitic copepod "probably of the genus *Parapetalus*" infecting the "gill" of yellowfin tuna [see Goto, [8]]) or type locality (western Pacific Ocean off Japan) since 1894. Goto's [8] original description of *C. biparasiticum* (as *Tristomum biparasiticum*) detailed the morphology of the genitalia, body, and accessory sclerites but subsequent descriptions were less complete, and, considering the lack of an extant holotype, the identity of most specimens ascribed to this species and collected from tunas remains indeterminate. Of the specimens identified as *C. biparasiticum* by the workers who published the original record, we know of only 3 extant specimens; all of which were vouchers collected from the dorsum of another putative species of parasitic copepod (*Elytrophora* sp., i.e., not a congener of the type host) that infected the buccal cavity of yellowfin tuna in the Pacific Ocean [10]. In addition to being from a copepod other than the type host, these specimens were minute compared to Goto's [8] description of *C. biparasiticum*; making for tenuous morphological comparisons between those sets of specimens. This discussion echos the concerns of Bussiéras and Baudin-Laurencin [42], and we remain uncertain about species boundaries within this group of closely-related capsalines that infect yellowfin tuna.

Distillation of these various taxonomic issues certainly justifies *C. biparasiticum* as a species of doubtful identity needing further investigation (*species inquirenda*), and this has systematic implications given that this taxon is the type species for *Caballerocotyla* Price, 1960 (considered a junior subjective synonym of *Capsala* by Chisholm and Whittington [7]). Noteworthy along these lines is that our phylogenetic analysis supported paraphyly of *Capsala*, which may be reflective of a distinct capsaline lineage comprising *Caballerocotyla* spp.

To identify the materials we collected from GOM yellowfin tuna but also to gain insights on potential species-level differences between putative specimens of "*C. biparasiticum*" that have been collected from the dorsum of parasitic copepods and from fish skin, we illustrated and gathered morphometric data from existing type and voucher materials for similar species of *Capsala* from the United States National Museum, Smithsonian Institution (USNM, Washington DC), Harold W. Manter Laboratory Parasite Collection (HWML, Lincoln, Nebraska), and the British Museum of Natural History (BMNH, London, England) (Table 1). Because these comparisons comprised a total of only 6 specimens (3 small adults from parasitic copepods and 3 larger adults from fish), collectively, we briefly summarize only those features that fell outside of the ranges we report for our specimens collected from GOM yellowfin tuna. These differences may likely be related to intraspecific variability, the niche on parasitic copepods, or ontogenetic differences among different-aged or -sized specimens. However, some do indicate species-level differences worthy of future investigation with morphology and molecular markers.

The holotype (Fig. 6) of *C. neothunni* (Yamaguti, 1968) was 4920 long × 2840 wide (body length without haptor). No value for any measured feature in the holotype of *C. neothunni* fell outside of the range that we reported above for the specimens we collected from GOM yellowfin tuna. These results seemingly support conspecificity of our specimens with this holotype.

The voucher specimens (Fig. 7) of *C. abidjani* (Bussiéras and Baudin-Laurencin, 1970) from "buccal cavity" of yellowfin tuna (BMNH Coll. Nos. 1975-9-17-11 and -12) (Table 1) were 4240 and 5280 long × 2360 and 3260 wide (body lengths without haptor). These specimens had a proportionally larger anterior attachment organ (15 and 16% of body width), seemingly fewer testes (86 and 90 total), testes that presented as deeply lobed (dendritic; testes stylized in Fig. 7), a testicular field that was proportionally shorter (38% and 35% of body length) but wider (33% and 42% of body width), and a proportionally shorter cirrus sac (4% of body width). As such, they appeared morphologically distinctive; however, we lacked enough comparative material to confidently assess if our specimens were conspecific with them or not. Chisholm and Whittington [7] and Barse and Bullard [20] emphasized the importance of dorsomarginal body sclerites in capsalid taxonomy. We observed some marked differences regarding dorsomarginal body sclerites among the specimens we studied (Figs. 10–14). The spacing of these sclerites seemed to differ among the specimens but the number of sclerites and their size were not markedly different. The specimens from parasitic copepods had the most dense arrangement of sclerites; whereas, those in specimens from tuna skin were more widely separated. The presence of numerous cusps in the dorsomarginal body sclerites of *Capsala* spp. is taxonomically meaningful, and we did not see any difference in the number of cusps among these specimens.

The voucher specimens (Fig. 8) of *C. biparasiticum* from the dorsum of parasitic copepods (*Elytrophora* sp.) (USNPC Coll. No. 38134 [2 vouchers]; HWML Coll. No. 44308 [1 voucher]) differed from the newly collected specimens by the following characters: (i) body size markedly smaller (1700–2420 long × 1720–1940 wide [body length without haptor]), (ii) diameter of anterior attachment organ proportionally larger (18–25% of maximum body width), (iii) body evenly rounded (body length/body width = 0.99–1.27) and lacking a marked diminution in breadth immediately posterior to the anterior suckers, (iv) haptor mostly ventral, i.e., not extending posteriad far beyond posterior body end (haptor posterior extension/body length = 0.04–0.12), (v) dorsomarginal body sclerites more closely spaced, (vi) testes smaller (60–80 in diameter), (vii) testicular field proportionally shorter (32–35% of body length) and wider (40–44% of body width), and (viii) vitellarium seemingly less developed, i.e., smaller, with follicles approximately 15–20 in diameter. Based on these observations, we speculate that these specimens were young adults (sexually mature but with gonads and genitalia less developed). We cannot know how old these specimens were or how long they were attached to the copepods before they were collected, and we also cannot discount completely the fact that these may represent a related species of *Capsala*.

Based only on the materials that we studied (including our newly collected specimens and existing museum materials sourced from fish and parasitic copepods), we concluded that (i) the capsalines from parasitic copepods are small (putatively young) adults, likely specimens that have not yet developed fully as compared to those collected from the skin of yellowfin tunas, (ii) the holotype of *C. neothunni*, Goto's [8] description of *C. biparasiticum*, and our specimens are morphologically similar, and (iii) *C. abidjani* warrants further investigation as a species distinct from *C. biparasiticum* and *C. neothunni*.

These taxonomic assessments based on morphology would obviously be greatly aided by the addition of molecular data from the nuclear small subunit ribosomal DNA (18S), nuclear large subunit ribosomal DNA (28S), and the internal transcribed spacer region of ribosomal DNA (ITS rDNA). Previous molecular taxonomic work has shown that at least one capsalid is potentially as widely distributed as its host tuna: Aiken et al. [1] sequenced 2 specimens of *Capsala* sp. (one from a southern bluefin tuna off Port Lincoln, Australia and another from a Pacific bluefin tuna off Mexico) and found them to be 100% identical in 28S

rDNA sequence. Aside from the present study, no molecular data exists for specimens identified as *C. biparasiticum* (see [1,6,22]), but rather obvious morphological differences, e.g., the proportional size, density, and distribution of the dorsomarginal body sclerites (Figs. 10–14), exist among specimens putatively identified as *C. biparasiticum* or that have been proposed as junior subjective synonyms of *C. biparasiticum*. Future molecular and morphological studies of additional capsalid specimens from parasitic copepods and from the fish hosts for those parasitic copepods could help test if Capsalidae includes a divergent lineage that has specialized on parasitic copepods, which may represent an evolutionary convergence among other monogenoids that infect parasitic crustaceans.

4.2. Copepods as capsaline hosts

It is highly unusual that a monogenoid naturally infects an invertebrate or that a monogenoid infects more than one host species during its life cycle [8,10,1,43–47]. Other monogenoids are facultative hyperparasites on ectoparasitic crustaceans (i.e., species of Diclidophoridae infecting parasitic isopods and the fish host of the infected isopod [44; personal observations SAB]) while still others are obligate hyperparasites of parasitic copepods (i.e., *Udonella* spp. that infect caligoid copepods [46,47]). However, other than for that of *Udonella* spp., very few or no biological details are available for monogenoids that have acquired invertebrates as hosts. Regarding specifically capsalines, aside from *C. biparasiticum* and *Capsala nozawae*, we are not aware of any other member of Capsalidae that is hyperparasitic or associated with an invertebrate host [7,48,49].

The presence of anterior pores and the size of the haptor may be influenced by attachment to the dorsum of a copepod or to fish skin. Regarding the anterior end (anterior pores), no previous account of a capsalid has documented the presence of anterior pores (Figs. 4, 6–9, 15, 16). We confirmed the presence of these pores in all materials examined herein, including specimens collected from parasitic copepods and tunas. We have not thoroughly investigated the function of these pores nor conducted the requisite ultrastructural studies for determining their anatomy; however, we suspect they secrete a biological adhesive. As at least some other species of *Capsala* clearly lack such pores and the associated mound of tegument that supports the pore (and perhaps encloses the adhesive gland), and because *C. biparasiticum* is a facultative hyperparasite of parasitic copepods, we wonder if these pores might be adaptive for infecting the dorsum of a parasitic copepod. Along these lines, confirming the presence/absence of these pores in *C. nozawae* (Goto, 1894) Price, 1938, which Yamaguti [11] reported to infect a "caligoid copepod parasitic in buccal cavity" of yellowfin tuna off Hawaii, would be interesting. Finally regarding these pores, their presence may be distinctive for *Caballerocotyla* (as *C. biparasiticum* is the type species of *Caballerocotyla*): these pores are apparently absent in *C. martinieri* (type species of *Capsala*).

Regarding the haptor, Bussiéras [13] designated two subspecies for *C. abidjani* based upon the presence of a strikingly small haptor in specimens (as *Caballerocotyla abidjani microcotyla*) collected from the inner surface of the operculum of yellowfin tuna and blackfin tuna, *Thunnus obesus*, captured in the eastern Atlantic Ocean (Table 1). The cephalothorax of parasitic copepods seemingly offers little space for attachment by large-bodied capsalines that each have a correspondingly large haptor, and Bussiéras's [13] observation of a small haptor may be related to the worm's habit of attaching to the copepod. Perhaps specimens having a small haptor proportional to body size have more recently switched from attachment to a copepod to attachment to the skin of a tuna. Large and small specimens of *C. biparasiticum* that have a proportionally small haptor have been reported from fishes and copepods (Table 1: Goto's [1894] specimens from the parasitic copepod had a body length and haptor diameter of 6 and 1.2 mm, respectively; those of Yamaguti [1968] from caligid copepods had 3.9–7.0 and 0.6–0.9 mm; and those of Yamaguti [1968] from fishes had 4.7–6.9 and 1.2–1.9). These data collectively indicate that this capsaline reaches its maximum reported length regardless of whether it is in association with a copepod or a fish (no relocation between hosts) or that (ii) it relocates from fish to copepod and visa versa. These intriguing matters also underscore the importance of reporting the anatomically explicit site of infection for *Capsala* spp. Many published works refer to "gill" as a site of infection; however, in the broad sense "gill" may include an array of structurally distinct micro-habitats to which monogenoids apparently show specificity: gill arch, respiratory surface of gill filaments, interlamellar water channels, buccal cavity epithelium, inner surface of the operculum, pseudobranch, etc.

4.3. Parasite–host relationship

Although particular capsalids (*Benedenia* spp.; *Neobenedenia* spp.) are notorious pathogens of marine fishes in net pens or recirculating aquaculture systems [50], very little information is available on how capsalids affect their free-ranging hosts in the epipelagic zone. For example, aside from the present study, we know of no detailed histopathological study that treats an infection by a species of *Capsala* in a wild-caught tuna or billfish. As a result, we lack fundamental insight on how these parasites affect their epipelagic hosts in nature (see also the pamphlet published by Rough, K. M. 2000. "An Illustrated Guide to the Parasites of Southern Bluefin Tuna, *Thunnus maccoyii*." Tuna Boat Owners Association of South Australia, Eastwood; cited in [3]). The pathological results of the present study indicate that *C.* cf. *biparasiticum* elicits a gross lesion on yellowfin tuna that comprises a thickening of the epidermis and extensive folding of epidermis and dermis near the parasite's feeding and attachment sites. The histological sections we examined lacked evidence of any deep, ulcerative wound or sign of secondary pathogen infection. Collectively, these histological observations conform to the intuitive and dogmatic view that ectoparasites and their fish hosts are typically in a sort of "equilibrium" such that the parasite infrapopulation persists on the wild fish host without causing significant deleterious physiological effects. For example, parasites of the infrapopulation feed on proliferating host cells but do not likely destroy the epidermis or make the underlying dermis vulnerable to bacterial infection or water logging and necrosis. As such, pathogenicity is related to infection intensity, which has been observed in aquaculture settings [50] and at least one field study wherein capsalid intensity was correlated with mortality of keeled mullets, *Liza carinata* (Valenciennes, 1836), in the Gulf of Suez [51,52]. That study was interesting and relevant because those authors postulated that oil contamination in the area was a contributing factor to high intensity infections and disease in the studied keeled mullets.

Regarding parasite feeding, areas of host skin beneath the anterior (oral) end of adult capsalid specimens was extensively rugose, blackish in color, and thickened. Given the seemingly limited number of possibilities for what tissue, extracellular components, or whole cells that these capsalines may feed upon, we speculate that the majority of their diet comprises components of the epidermis, e.g., malpighian cells and goblet cells. As indicated for other monogenoids that infect fish skin [53], specimens of *C.* cf. *biparasiticum* would thereby gain access to a continuous source of regenerating host cells at their attachment site. Adults of *C.* cf. *biparasiticum* were haphazardly oriented, indicating that worms pivot about the haptoral attachment site; enabling them to feed on adjacent sites or contact conspecific worms.

4.4. Assessing Gulf of Mexico fish lesions

The northern GOM's outer continental shelf is the largest open area for offshore energy exploration in the continental US and includes an extensive network of deepwater oil rigs (outer continental shelf tension leg platforms, OCS-TLPs). In addition to extracting oil and gas, OCS-TLPs attract and hold diverse fish communities [54,55]. This same sector of the GOM, also referred to historically as the "Fertile Fisheries Crescent"

[56], is among the world's richest fishing grounds and critical habitat for highly migratory yellowfin tuna [54,55]. Yellowfin tuna historically have aggregated on drowned reef complexes and salt domes but an ecological shift has occurred wherein tunas and other pelagic apex predators aggregate about OCS-TLPs [57]. Although we are aware of no epidemiological study that has been published, OCS-TLPs may affect fish parasite transmission and subsequent host population and disease dynamics. Toxicants can be associated with drilling activities [58–60], and some evidence supports the notion that fish associating with active drilling platforms can experience deleterious health effects. For example, in relatively shallow water zones in the GOM, Grizzle [61] reported that the livers of several fishes collected near oil platforms were significantly larger than those of conspecifics captured from a control site. In addition, some fishes near oil platforms had more frequent gill lesions and a higher prevalence of liver fatty change. Fish exposed to toxicants theoretically may be more susceptible to infectious disease, and, hence, a nuanced understanding of the abiotic environment and parasite–host relationships could contribute to our understanding of fish health within OCS-TLP fish communities. The recent Gulf of Mexico oil spill (DHOS; [62,63]) heightened awareness of fish health in the GOM's OCS. Given the known biodiversity of parasites and pathogens that infect GOM fishes (e.g., [64,65]) and their ability to be associated with gross lesions on fishes (e.g., [53,66–68]; present study), lesion etiology should be informed by parasitology and pathology so as to avoid overly simplistic and/or erroneous explanations of observed fish abnormalities and lesions.

Acknowledgments

We thank Marianna Bradley, Monty Simmons, Clint Edds, and Myron Fischer (Louisiana Department of Wildlife and Fisheries; Marine Fisheries Laboratory, Grand Isle, Louisiana) for variously facilitating fish collection logistics off Louisiana. We thank Eric Hoberg and Pat Pilitt (both United States National Parasite Collection, Beltsville, Maryland), Scott Gardner (Harold W. Manter Laboratory of Parasitology, Lincoln, Nebraska), and Eileen Harris (Natural History Museum, London, UK) for loaning relevant capsalid specimens. We thank Kirsten Rough (Australian Southern Bluefin Tuna Industry Association, Port Lincoln, Australia) for emailing a PDF of her field identification booklet detailing capsalid infections. This is a contribution of the Center for Aquatic Surveillance and Health (CASH) (including the Southeastern Cooperative Fish Parasite and Disease Project), School of Fisheries, Aquaculture, and Aquatic Science, and was supported in part by Gulf of Mexico Research Initiative and National Science Foundation grants to SAB.

References

[1] H.M. Aiken, N.J. Bott, I. Mladineo, F.E. Montero, B.F. Nowak, C.J. Hayward, Molecular evidence for cosmopolitan distribution of platyhelminth parasites of tunas (*Thunnus* spp.), Fish 8 (2007) 167–180.
[2] J. Culurgioni, S. Mele, P. Merellla, V. Addis, A. Figus, F. Cau, et al., Metazoan gill parasites of the Atlantic bluefin tuna, *Thunnus thynnus* (Linnaeus) (Osteichthyes: Scombridae) from the Mediterranean and their possible use as biological tags, Folia Parasitol. 61 (2) (2014) 148–156.
[3] B.L. Munday, Y. Sawada, T. Cribb, C.J. Hayward, Diseases of tunas, *Thunnus* spp. J. Fish Dis. 26 (2003) 187–206.
[4] I. Mladineo, J. Žilić, M. Čanković, Health survey of Atlantic bluefin tuna, *Thunnus thynnus* (linneaus, 1758), reared in Adriatic cages from 2003 to 2006, J. World Aquacult. Soc. 39 (2) (2008) 281–289.
[5] E.J. Peeler, N.G.H. Taylor, The application of epidemiology in aquatic animal health — opportunities and challenges, Vet. Res. 42 (2011) 94–109.
[6] I.D. Whittington, The Capsalidae (Monogenea: Monopisthocotylea): a review of diversity, classification and phylogeny with a note about species complexes, Folia Parasitol. 51 (2004) 109–122.
[7] L.A. Chisholm, I.D. Whittington, Review of the Capsalinae (Monogenea: Capsalidae), Zootaxa 1559 (2007) 1–30.
[8] S. Goto, Studies on the ectoparasitic trematodes of Japan, J. Coll. Sci. Imp. Univ. Tokyo 8 (1894) 1–273.
[9] E.W. Price, North American monogenetic trematodes III. The family Capsalidae (Capsaloidea), J. Wash. Acad. Sci. 29 (1939) 63–92.
[10] E.S. Iverson, E.E. Hoven, Some trematodes of fishes from the central equatorial Pacific, Pac. Sci. 12 (1958) 131–134.
[11] S. Yamaguti, Monogenetic Trematodes of Hawaiian Fishes, University of Hawaii Press, Hawaii, 1968 (287 pp.).
[12] J. Bussiéras, F. Baudin-Laurencin, *Caballerocotyla abidjani* n. sp. (Monogenea: Capsalidae), parasite des opercules du thon albacore, *Thunnus albacares*, Cahiers Office de la Recherche Scientifique et Technique Outre, Série Océanographie, 31970 47–51.
[13] J. Bussiéras, Les Monogènes Capsalinae parasites des thons de l'Atlantique tropical oriental, Ann. Parasitol. (Paris) 47 (1972) 29–49.
[14] G. Vassiliadès, Helminthes parasites des poissons de mer des cotes du Senegal, Bulletin de l'Institute Fondamental d'Afrique Noire, 44(1-2)1985 78–99 (French).
[15] S.E. Pozdnyakov, Helminths of Scombrid-like Fishes of the World's Oceans, DVO AN SSSR, Vladivostok, 1990 [in Russian].
[16] T.P. Egorova, 'Occurrence of monogeneans of the superfamily Capsalinae (Capsalidae) parasites of marine fishes'. Parazitologiya. Akademiya Nauk SSSR, Leningrad 34 (2) (2000) 111–117 (in Russian).
[17] A. Kohn, M.C.N. Justo, *Caballerocotyla llewelyni* n. sp. and *Caballerocotyla neothunni* (Yamaguti, 1968) (Monogenea: Capsalidae) parasites of Brazilian tunas (Scombridae), Zootaxa 1139 (2006) 19–26.
[18] B.B. Collette, Scombridae (mackerels and tunas), in: K. Carpenter (Ed.), FAO Species Identification Guide for Fishery Purposes, the Living Marine Resources of the Western Central Atlantic, Bony Fishes Part 2 (Opistognathidae to Molidae), Sea Turtles and Marine Mammals, vol. 3, FAO, Rome, Italy 2002, pp. 1836–1859.
[19] S.A. Bullard, R. Payne, J.S. Braswell, New genus with two new species of capsalid monogeneans from dasyatids in the Gulf of California, J. Parasitol. 90 (6) (2004) 1,412–1,427.
[20] A.M. Barse, S.A. Bullard, Redescription and new host record of *Capsala laevis* (Capsalinae) from roundscale spearfish, *Tetrapturus georgii* (Perciformes: Istiophoridae) in the northwestern Atlantic Ocean, J. Parasitol. 98 (4) (2012) 735–745.
[21] L.A. Chisolm, J.A.T. Morgan, R.D. Adlard, I.D. Whittington, Phylogenetic analysis of the Monocotylidae (Monogenea) inferred from 28S rDNA sequences, Int. J. Parasitol. 31 (2001) 1253–1263.
[22] E.M. Perkins, S.C. Donnellan, T. Bertozii, L.A. Chisholm, I.D. Whittington, Looks can deceive: molecular phylogeny of a family of flatworm ectoparasites (Monogenea: Capsalidae) does not reflect current morphological classification, Mol. Phylogenet. Evol. 52 (2009) 705–714.
[23] K. Katoh, H. Toh, Parallelization of the MAFFT multiple sequence alignment program, Bioinformatics 26 (15) (2010) 1899–1900.
[24] M.A. Miller, W. Pfeiffer, T. Schwartz, Creating the CIPRES Science Gateway for inference of large phylogenetic trees, Proceedings of the Gateway Computing Environments Workshop (GCE), New Orleans, Louisiana 2010, pp. 1–8.
[25] K. Tamura, D. Peterson, N. Peterson, G. Stecher, M. Nei, S. Kumar, MEGA5: molecular evolutionary genetics analysis using maximum likelihood, evolutionary distance, and maximum parsimony methods, Mol. Biol. Evol. 28 (2011) 2731–2739.
[26] J. Castresana, Selection of conserved blocks from multiple alignments for their use in phylogenetic analysis, Mol. Biol. Evol. 17 (2000) 540–552.
[27] D. Posada, T.R. Buckley, Model selection and model averaging in phylogenetics: advantages of Akaike Information Criterion and Bayesian approaches over likelihood ratio tests, Syst. Biol. 53 (2004) 793–808.
[28] D. Darriba, G.L. Taboada, R. Doallo, D. Posada, jModelTest 2: more models, new heuristics and parallel computing, Nat. Methods 9 (2012) 772.
[29] S. Guindon, O. Gascuel, A simple, fast and accurate method to estimate large phylogenies by maximum-likelihood, Syst. Biol. 52 (2003) 696–704.
[30] J.P. Huelsenbeck, R. Ronquist, Bayesian analysis of molecular evolution using MrBayes, in: R. Nielsen (Ed.), Statistical Methods in Molecular Evolution, SpringerVerlag, New York, USA 2005, pp. 183–232.
[31] J.P. Huelsenbeck, F. Ronquist, R. Nielsen, J.P. Bollback, Bayesian inference of phylogeny and its impact on evolutionary biology, Science 294 (2001) 2310–2314.
[32] F. Ronquist, J.P. Huelsenbeck, MRBAYES 3: Bayesian phylogenetic inference under mixed models, Bioinformatics 19 (2003) 1572–1574.
[33] A. Rambaut, A.J. Drummond, Tracer Version 1.5. Program, 2009 (Available from: http://beast.bio.ed.ac.uk/Tracer/).
[34] A. Rambaut, FigTree v1.2.3, Institute of Evolutionary Biology, Univ. of Edinburgh, 2009 (Available at http://tree.bio.ed.ac.uk/software/figtree).
[35] W.N. Eschmeyer, Catalog of fishesAccessed 9 February 2015 http://research.calacademy.org/ichthyology/catalog.
[36] W.N. Eschmeyer, J.D. Fong, Species of fishes by family/subfamilyOn-line version dated 3 Feb 2015 http://research.calacademy.org/research/ichthyology/catalog/SpeciesByFamily.asp.
[37] J.S. Nelson, Fishes of the World, 4th edition John Wiley and Sons, Inc., New York, 2006 601.
[38] L.A. Chisholm, I.D. Whittington, Revision of *Capsaloides* (Monogenea: Capsalidae) with a redescription of *C. magnaspinosus* Price, 1939 from the nasal tissue of *Tetrapterus audax* (Istiophoridae) collected off Nelson Bay, New South Wales, Australia, Zootaxa 1160 (2006) 1–20.
[39] International Commission on Zoological Nomenclature, International Code of Zoological Nomenclature, 4th ed. International Trust for Zoological Nomenclature, London, UK, 2015 (306 pp.).
[40] S.A. Bullard, O. Olivares-Fuster, G.W. Benz, C.R. Arias, Molecules infer origins of ectoparasite infracommunities on tunas, Parasitol. Int. 60 (2011) 447–451.
[41] R. Dollfus, Deuz espèces de trématodes monogénétiques parasites du "bluefin tuna" de Californie, 1962.
[42] J. Bussiéras, F. Baudin-Laurencin, Les helminthes parasites des thons tropicaux, Revue d'Élevage et de Médicine Vétérinaire des Pays Tropicaux, 261973 13a–19a.

[43] N. Sproston, A contribution to the ecology of the *Capsala* on the southern bluefin tuna (*Thunnus maccoyi*), Parazitologicheskii sbornik, 241969 242–243.
[44] R.M. Overstreet, Metazoan symbionts of crustaceans, in: A.J. Provenzano (Ed.) The Biology of Crustacea: Pathobiology, vol. 6, Academic Press, Inc., New York, New York 1983, pp. 155–250 (Chapter 4).
[45] S.A. Bullard, G.W. Benz, J.S. Braswell, *Dionchus* postoncomiracidia (Monogenea: Donchidae) from the skin of blacktip sharks, *Carcharhinus limbatus* (Carcharhinidae), J. Parasitol. 86 (2) (2000) 245–250.
[46] G.W. Benz, S.A. Bullard, Chapter 24: metazoan parasites and associates of chondrichthyans with emphasis on taxa harmful to captive hosts, in: M.F.L. Smith, D.A. Thoney, R.E. Hueter (Eds.),The Husbandry of Elasmobranch Fishes. Columbus, OH: Special Publication No. 16, Ohio Biological Survey 2004, pp. 325–416.
[47] M.A. Freeman, K. Ogawa, Variation in the small subunit ribosomal DNA confirms that *Udonella* (Monogenea: Udonellidae) is a species rich group, Int. J. Parasitol. 40 (2010) 255–264.
[48] A.R. Lawler, Zoogeography and host-specificity of the superfamily Capsaloidea Price, 1936 (Monogenea: Monopisthocotylea). An evaluation of the host–parasite records of the superfamily Capsaloidea Price, 1936, and their utility in determinations of host-specificity and zoogeography, Special Publications in Marine Science, 6, Virginia Institute of Marine Science, Virginia, U.S.A., 1981 (650 pp.).
[49] R. Lamothe-Argumedo, Nuevo arreglo taxonómico de la subfamilia Capsalinae (Monogenea: Capsalinae), clave para los géneros y dos combinaciones nuevas, Anales del Instituto de Biología, Universidad Nacional Autónoma de México, Serie Zoologia, 681997 207–223.
[50] I.D. Whittington, L.A. Chisholm, Diseases caused by Monogenea, in: J. Eiras, H. Segner, T. Wahil, B.G. Kapoor (Eds.), Fish Diseases, Science Publishers, Enfield, New Hampshire 2008, pp. 817–976.
[51] I. Paperna, R.M. Overstreet, Parasites and diseases of mullets (Mugilidae), in: O.H. Oren (Ed.) Aquaculture of Grey Mullets, International Programme, 26, Cambridge University Press, Cambridge 1981, pp. 411–493.
[52] I. Paperna, A. Diamant, R.M. Overstreet, Monogenean infestations and mortality in wild and cultured Red Sea fishes, Helgoländer Meeresuntersuchungen, 371984 445–462.
[53] S.A. Bullard, S. Frasca Jr., G.W. Benz, Skin lesions caused by *Dermophthirius penneri* (Monogenea: Microbothriidae) on wild-caught blacktip sharks (*Carcharhinus limbatus*), J. Parasitol. 86 (3) (2000) 618–622.
[54] R.L. Hiett, J.W. Milon, Economic Impacts of Recreational Fishing and Diving Associated With Offshore Oil and Gas Structures in the Gulf of Mexico (Final Report, OCS Study MMS 2002-010), US Department of the Interior, Minerals Management Service, Gulf of Mexico OCS Region, New Orleans, 2010 (March 2002, 70 pages).
[55] A. Scarborough-Bull, M.S. Love, D.M. Schroeder, Artificial reefs as fishery conservation tools: contrasting the roles of offshore structures between the Gulf of Mexico and the Southern California Bight, Am. Fish. Soc. Symp. (2006) 1–18.
[56] G. Gunter, The fertile fisheries crescent, J. Miss. Acad. Sci. 9 (1963) 286–290.
[57] J.P. Hoolihan, R.J.D. Wells, J. Luo, B. Falterman, E.D. Prince, J.R. Rooker, Vertical and horizontal movements of yellowfin tuna in the Gulf of Mexico, Mar. Coast. Fish. 6 (2014) 211–222.
[58] B.M. Dicks, Environmental impact of North Sea oil platforms, The Marine Environment and Oil Facilities, Institution of Civil Engineers, London 1979, pp. 1–12.
[59] J.B. Sprague, W.J. Logan, Separate and joint toxicity to rainbow trout of substances used in drilling fluids for oil exploration, Environ. Pollut. 9 (1979) 269–281.
[60] W.E. Haensly, J.M. Neff, J.R. Sharp, A.C. Morris, M.F. Bedgood, P.D. Boem, Histopathology of *Pluronetes patessa* L. from Aber Warc'h and Aber Benoit, Brittany, France. Long-term effects of the *Amoco Cadiz* crude oil spill, J. Fish Dis. 5 (1982) 365–391.
[61] J.M. Grizzle, Lesions in fishes captured near drilling platforms in the Gulf of Mexico, Mar. Environ. Res. 18 (1986) 267–276.
[62] J. Lubchenco, M. McNutt, G. Dreyfus, S.A. Murawski, D. Kennedy, P. Anastas, et al., Science in support of the Deepwater Horizon response—an introduction, Proc. Natl. Acad. Sci. U. S. A. 109 (2012) 20212–20221.
[63] M. McNutt, S. Chu, J. Lubchenco, T. Hunter, G. Dreyfus, S.A. Murawski, et al., Applications of science and engineering to quantify and control the Deepwater Horizon oil spill, Proc. Natl. Acad. Sci. U. S. A. 109 (2012) 20222–20228.
[64] K. Jensen, Cestoda (Platyhelminthes) of the Gulf of Mexico, in: D.L. Felder, D.K. Camp (Eds.), Gulf of Mexico; Origin, Waters, and Biota, Biodiversity, vol. 1, Texas A&M University Press, College Station, Texas 2009, pp. 487–522.
[65] R.M. Overstreet, J.O. Cook, R.W. Heard, Trematoda (Platyhelminthes) of the Gulf of Mexico, in: D.L. Felder, D.K. Camp (Eds.), Gulf of Mexico; Origin, Waters, and Biota, Biodiversity, vol. 1, Texas A&M University Press, College Station, Texas 2009, pp. 419–486.
[66] J. Borucinska, S.A. Bullard, Lesions associated with pleurocerci (Platyhelminthes: Cestoda: Trypanorhyncha) in the gastric wall of a cownose ray, *Rhinoptera bonasus* (Myliobatiformes: Rhinopteridae) from the Northern Gulf of Mexico, J. Fish Dis. 34 (2011) 149–157.
[67] C.F. Ruiz, C. Ray, M. Grace, M. Cook, S.A. Bullard, A new species of Trichosomoididae (Nematoda) from skin of red snapper, *Lutjanus campechanus* (Perciformes: Lutjanidae), on the Texas–Louisiana shelf, Northern Gulf of Mexico, J. Parasitol. 99 (2) (2013) 318–326.
[68] C.F. Ruiz, S.A. Bullard, *Huffmanela markgracei* sp. n. (Nematoda: Trichosomoididae) from buccal cavity of Atlantic sharpnose shark, *Rhizoprionodon terraenovae* (Carcharhiniformes: Carcharhinidae), in the northwestern Gulf of Mexico off Texas, Folia Parasitol. 60 (4) (2013) 353–358.